2. Laminar Premixed Flame Study

2.1 Introduction

One-dimensional laminar premixed flames are attractive for studying soot formation because they involve simple flows that promote the tractability of both measurements and detailed numerical simulations needed to evaluate soot formation models. These observations have motivated numerous studies of soot formation in burner-stabilized laminar premixed flames, see Refs. 1-16 and references cited therein. Nevertheless, burner-stabilized laminar premixed flames are problematical for studies of soot formation for a number of reasons: spatial resolution and residence times are limited at the pressures typical of many practical applications, flame structure is sensitive to minor burner construction details so that experimental reproducibility is not very good; consistent burner behavior over the lengthy test programs needed to define soot formation properties is hard to achieve; burners have poor durability at pressures typical of many practical applications; it is difficult to quantify conductive, convective and radiative heat losses to the burner; it is difficult to define flow velocities near the burner where the flow is multidimensional and velocities change rapidly with streamwise distance due to effects of buoyancy; such flames are hard to seed for nonintrusive measurements of velocities and scalar properties; and it is difficult to carry out fundamental numerical simulations of premixed flame properties due to multidimensional effects and the complex geometries of flame holders, e.g., porous plates, [9-16]. Many of these problems are mitigated, however, for soot-containing outwardly-propagating spherical laminar premixed flames which offer a flow configuration that is tractable for measurements and computations with a durable and easily reproducible experimental arrangement. Thus, the objective of the present investigation was to determine both the properties of these flames and their potential for studying soot formation in premixed flame environments.

Several issues must be considered when contemplating the use of outwardly-propagating spherical laminar premixed flames for studies of soot formation, as follows: (1) what conditions are required for these flame to contain soot? (2) what are the potential limitations of preferential-diffusion/stretch interactions that are known to modify the properties of these flames? and (3) what are the potential limitations imposed by the various instabilities (preferential diffusion, hydrodynamic and buoyant) known to affect these flames? The sooting limit, defined as the critical fuel-equivalence ratio where soot first appears in laminar premixed flames, is an important parameter that provides insight about the propensity of particular fuels to soot. Thus, a number of workers have measured sooting limits for premixed flames stabilized on burners at atmospheric pressure, and this information has been used to evaluate soot formation models, see Refs. 17-22 and references cited therein. Corresponding information about sooting limits for

outwardly-propagating laminar premixed flames, which avoid effects of burner heat losses, and about effects of pressure on sooting limits, however, have not been reported.

Effects of preferential-diffusion/stretch interactions on the properties of laminar premixed flames have received significant attention since the pioneering work of Law and his associates [23]. Recent studies along these lines for outwardly-propagating laminar premixed flames can be found in Refs. 24-38 and references cited therein. A surprising feature of these findings is that preferential-diffusion/stretch interactions cause large (ca. 100%) variations of laminar burning velocities, even well away from extinction conditions, for conventional hydrocarbon air mixtures that are of interest for studies of soot processes. Such behavior can cause problems of preferential-diffusion instability, which could limit the value of outwardly-propagating flames for soot formation studies. Hydrodynamic and buoyant instabilities can create similar problems. Unfortunately, little is known about the conditions when these instabilities are present for soot-containing outwardly-propagating spherical laminar premixed flames.

The objectives of the present investigation were to help fill the gaps in the literature that were just discussed concerning sooting limits and the stability of outwardly-propagating spherical laminar premixed flames at conditions potentially useful for studying soot formation in laminar premixed flame environments. The study involved completing new measurements of these properties, considering ethylene, ethane, propylene, 1-3 butadiene and propane burning in air at normal temperature and pressures of 0.5 - 4.0 atm.

2.2 Experimental Methods

The experiments were carried out in a spherical chamber used during earlier studies of flame/stretch interactions of outwardly-propagating spherical laminar premixed flames in this laboratory [24-30]. A sketch of the test arrangement appears in Fig. 1. The chamber had a volume of 0.024 m^3 and an inside diameter of 360 mm. Optical access was provided by two 100 mm diameter windows mounted opposite one another along a horizontal optical axis passing through the center of the chamber. Only conditions having flame diameters less than 60 mm (comprising roughly 0.5% of the chamber volume) were considered so that pressure increases during flame propagation were less than 0.7% and could be ignored.

The reactant mixtures were prepared within the chamber by adding gases at appropriate partial pressures to reach the desired test pressure. The gases were then mixed using a small electrical fan within the test chamber. All motion of the test gas during mixing was allowed to decay before the gas mixture was ignited. After combustion was complete, the chamber was vented to the laboratory exhaust system and then purged with dry air to remove condensed water vapor before refilling for the next test.

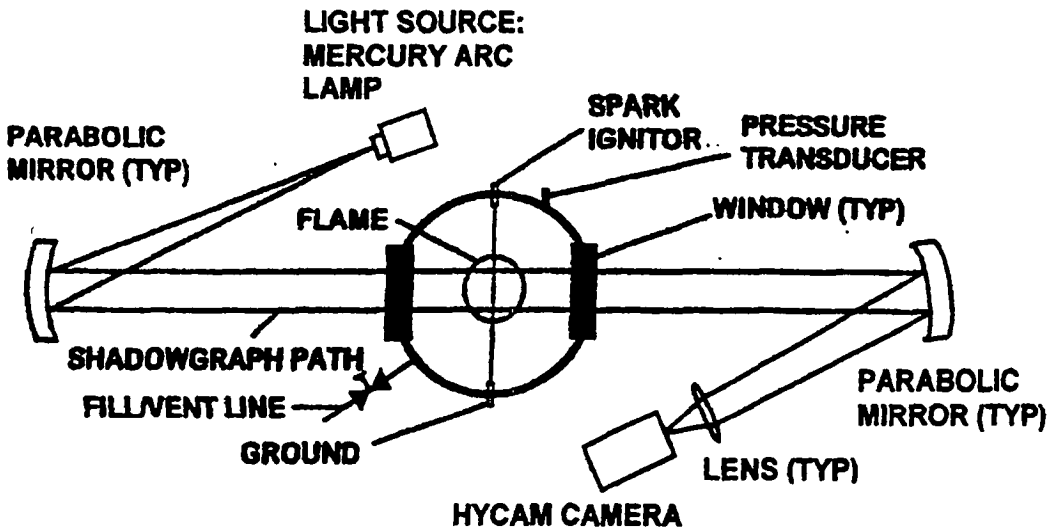

Fig. 1. Sketch of the test apparatus for observing outwardly-propagating laminar premixed flames.

The combustible mixture was spark ignited at the center of the chamber using electrodes extending along an axis at 45° to the vertical. The spark energy was supplied by a high-voltage capactor discharge circuit yielding spark energies of 5 - 20 mJ with a discharge time of roughly 5 μs. Near minimum ignition energies were used in order to minimize ignition disturbances.

The measurements involved observing the flames using both black and white motion picture shadowgraphs and color video records. The shadowgraph system is sketched in Fig. 1 and is described by Hassan et al. [27]; therefore, this information will not be repeated here. The video system was based on a Panasonic color digital camera (WV-CL352) which was triggered so that the flames could be recorded when they reached the desired size; exposure times were in the range 1 - 4 ms to stop flame motion on the film.

2.3 Flame Propagation Properties

Definition of test conditions must account for preferential-diffusion/stretch interactions and flame surface instabilities. This involves variations of laminar burning velocities with flame stretch that can be characterized using an early proposal of Markstein, as follows [24-27]:

$$S_L = S_{L\infty} - LK \tag{1}$$

After representing characteristic flame length and time scales by the local values of stretched flames, Eq. (1) can be placed in dimensionless form, as follows [24]:

$$S_{L\infty}/S_L = 1 + Ma\ Ka \tag{2}$$

A convenient feature of this approach is that Ma is relatively independent of Ka, which simplifies reporting of flame/stretch interactions.

Another useful property of Ma is that it provides a direct indication of the preferential-diffusion stability of flame surfaces. For example, $Ma < 0$ ($Ma > 0$) implies that concave disturbances directed toward the unburned gas of an otherwise plane flame surface, which have $Ka > 0$ similar to outwardly-propagating premixed flames, have increased (decreased) values of S_L compared to the $S_{L\infty}$ of the plane flame surface so that the disturbance grows (decays) and the flame is unstable (stable) [24-27].

Determinations of S_L were based on measurements of flame radius as a function of time for conditions where values of δ_f/r_f were small so that effects of flame curvature and unsteadiness are small. Effects of radiative heat loss within the premixed flame sheet were also ignored while

adopting the convention of ignoring effects of Ka on ρ_b [26,27]. Under these assumptions, Strehlow and Savage [28] show that S_L and K can be found as follows:

$$S_L = (\rho_b/\rho_u)dr_f/dt, \quad K = (2/r_f)\, dr_f/dt \tag{3}$$

In Eq. (3), ρ_b/ρ_u is found for an unstretched adiabatic flame in the reactant mixture at initial test chamber conditions while assuming chemical equilibrium in the combustion product mixture using the Gordon and McBride code, see Refs. 26 and 27. From Eq. (3) it is clear that Ka progressively decreases as r_f increases for outwardly-propagating premixed flames, tending to reduce variations of burned gas properties with distance behind the flame sheet due to preferential-diffusion/stretch interactions.

2.4 Buoyant Stability

Soot-containing laminar premixed flames have relatively large fuel-equivalence ratios and thus relatively small laminar burning velocities and flame speeds [27-36]. As a result, flame distortion by buoyancy becomes problematical which introduces flame stretch effects that are difficult to quantify. It was found that conditions where buoyancy was significant could be characterized by a buoyancy ratio, R, defined as the ratio of the characteristic buoyant velocity, defined as follows:

$$u = (2gr_f\,(\rho_u - \rho_b)/\rho_u)^{1/2} \tag{4}$$

and the laminar flame speed, dr_f/dt. Then introducing Eq. (3) for the laminar flame speed, the buoyancy ratio becomes

$$R = (2g\, r_f(\rho_u - \rho_b)/\rho_u)^{1/2}/((\rho_u/\rho_b)S_L) \tag{5}$$

Observations of present flames suggest that flame distortion by buoyancy becomes small when $R < 0.5$.

2.5 Results and Discussion

Flow Visualization. Black and white images of the color video records are considered in the following in order to illustrate flame surface properties due to effects of preferential-diffusion and buoyant instability. Flame color taken from the video records will also be noted in order to relate stability and sooting limits. It should also be noted at the outset that all hydrocarbon/air mixtures considered here exhibit preferential -diffusion instabilities at fuel-rich conditions, and that all the present soot-containing flames were in the region of potential preferential-diffusion

instability (i.e., Ma $\leq$ 0). Thus the appearance of preferential-diffusion instability for present soot-containing flames was largely decided by the degree to which a chaotically disturbed flame surface developed over the region of observation of the flames ($r_f \leq 30$ mm). Finally, it should be noted that cellular disturbances associated with hydrodynamic instabilities were observed at $r_f > 30$ mm for stable preferential-diffusion conditions, similar to past work [24-38], however, these flames were soot-free and this instability mechanism will not be considered any further here.

Typical photographs of stable soot-free ($\phi = 1.75$) and soot-containing ($\phi = 2.00$) flames used to define sooting limits are illustrated in Fig. 2. These results are for ethylene/air flames at atmospheric pressure for flame radii of roughly 30 mm. The flame on the left for $\phi = 1.75$ was entirely blue while the flame on the right for $\phi = 2.00$ had a blue outer edge shortly followed by a yellow region caused by continuum radiation from soot particles (seen as a second luminous boundary in the flame on the right). As noted earlier, both these flames are in the preferential-diffusion unstable region where Markstein numbers are negative (Ma $\approx$ -0.7 and -2.3 for $\phi = 1.75$ and 2.00 by extrapolation of the measurements of Ref. 27) which accounts for the persistence of flame surface disturbances due to the spark electrodes that are very evident in the photograph of the $\phi = 1.75$ flame. Nevertheless, chaotic disturbances of the flame surface due to preferential-diffusion instabilities develop relatively slowly for these modestly negative values of Ma and the small flame speeds at fuel-rich conditions, particularly at low pressures, and they have not yet appeared for these flames (although they do eventually appear when $r_f > 30$ mm).

Typical photographs of unstable soot-free ($\phi = 1.50$) and soot-containing ($\phi = 2.00$) flames used to define sooting limits are illustrated in Fig. 3. These results are for ethylene/air flames at 4 atm for flame radii of roughly 30 mm. The flame on the left for $\phi = 1.50$ was entirely blue while the flame on the right for $\phi = 2.00$ has a barely visible blue boundary that rapidly evolved to a yellow color caused by continuum radiation from soot. Both these flames are in the preferential-diffusion unstable region (Ma $\approx$ -9.3 and -10.6 for $\phi = 1.50$ and 2.00 by extrapolation of the measurements of Ref. 27) and both exhibit chaotic distortion of the flame surface that is characteristic of preferential-diffusion instability for these 60 mm diameter flames. It should be noted, however, that the presence of yellow luminosity due to continuum radiation from soot was generally evident before the flame surface became disturbed so that the presence of preferential-diffusion instability did not affect determination of the sooting limit. Finally, the distortion of the flame surface appears sooner in Fig. 3 than in Fig. 2 due to the much larger negative values of Ma and a tendency for flame surface disturbances to grow faster as the pressure was increased.

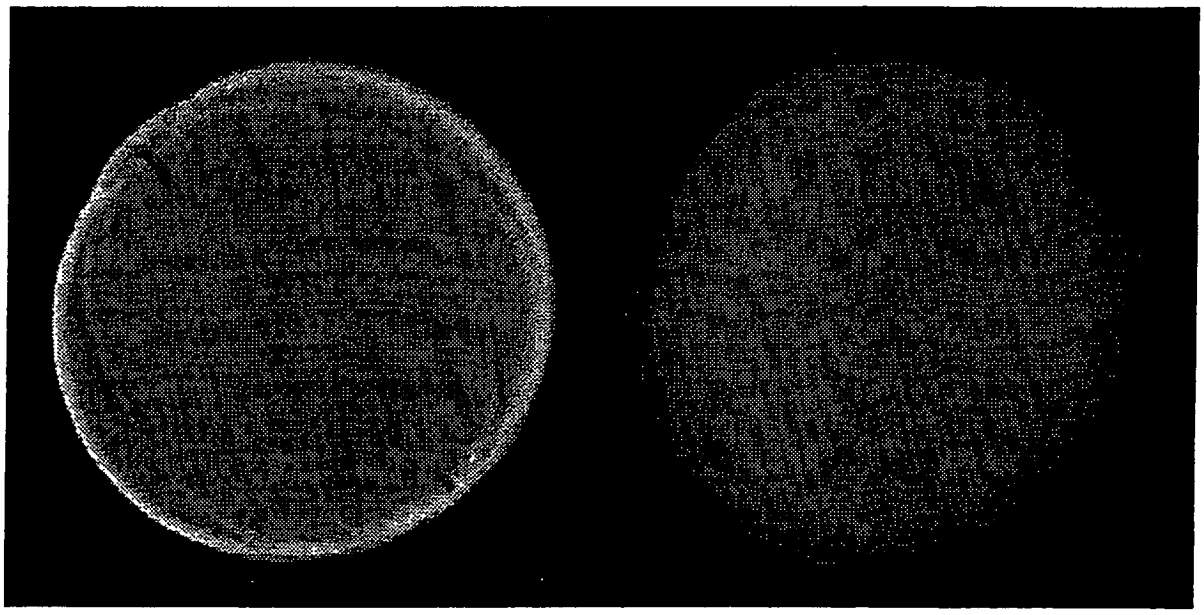

Fig. 2. Photographs of preferential-diffusion stable soot-free (ϕ=1.75) and soot-containing (ϕ=2.00) outwardly-propagating spherical laminar premixed flames (ethylene/air at 1 atm.).

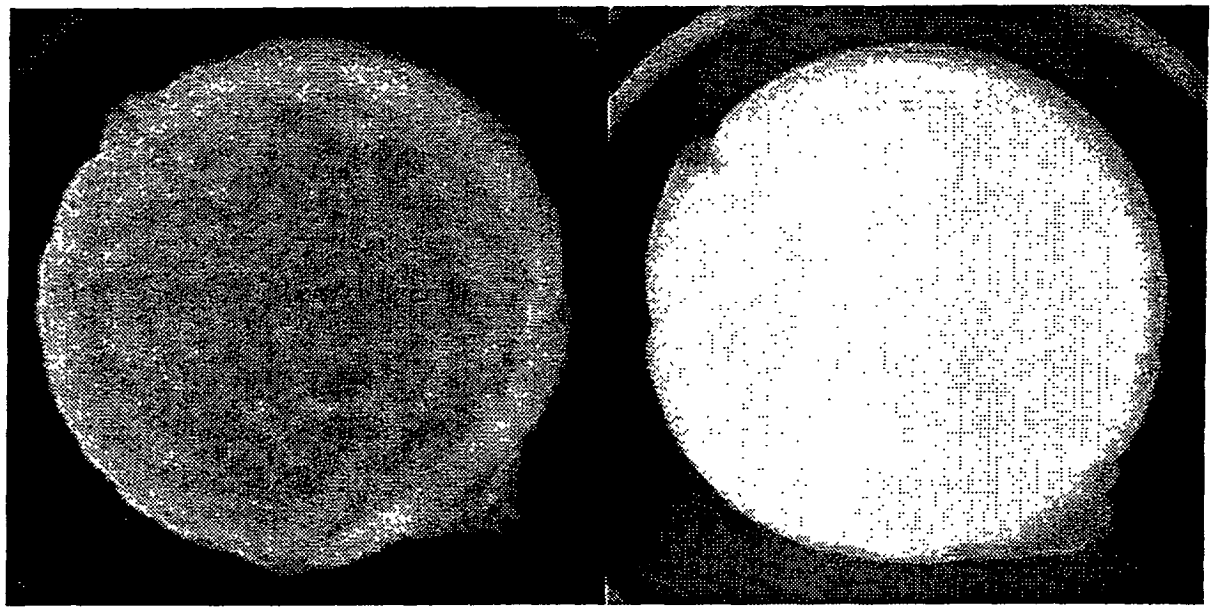

Fig. 3. Photographs of preferential-diffusion unstable soot-free (ϕ=1.50) and soot-containing (ϕ=2.00) outwardly-propagating spherical laminar premixed flames (ethylene/air at 4 atm.).

Photographs of the development of a soot-containing flame (ϕ = 1.75) having significant buoyant disturbances are illustrated in Fig. 4. In this case the images all are yellow due to the presence of continuum radiation from soot. These results are for an ethane/air flame at 4 atm which implies Ma = -9.9 by extrapolation of the measurements of Ref. 27 and R = 2.6 (when r_f = 30 mm); therefore, this flame is within the region subject to both strong preferential-diffusion and strong buoyant instabilities (Ma << 0 and R >> 0.5). In fact, the flame does exhibit both modes of instability along with effects of Rayleigh-Taylor *stability*. For example, the first two images of the flame exhibit chaotic flame surface disturbances that are characteristic of preferential-diffusion instability. The second image, however, also exhibits flame surface distortion with the bulk of the flame rising toward the top of the chamber, which is characteristic of buoyant instabilities. An interesting feature of the second and subsequent photographs, however, is that chaotic disturbances are not present along the bottom of the flame due to Rayleigh-Taylor *stability* (the stability of an interface when a less dense fluid is accelerated toward a more dense fluid). All these disturbances, combined with problems of estimating stretch effects in the period where the flame is small and the chamber pressure is nearly constant, imply that buoyant flames typical of conditions illustrated in Fig. 4 are not very attractive for studying soot formation processes.

Sooting and Stability Limits. Observations of sooting and stability limits are illustrated for outwardly-propagating spherical laminar premixed ethylene, ethane, proplyene, propane and 1 -3 butadiene/air flames in Figs. 5-9, respectively. Properties illustrated on these plots include the critical fuel-equivalence ratio as a function of pressure at the sooting limit, the buoyant limit (based on R = 0.5 as noted earlier), the fundamental preferential-diffusion stability limit (Ma = 0) drawn from the measurements of Hassan et al.[27], the actual preferential-diffusion stability limit based on the presence of a chaotically disturbed flame surface for $r_f \leq 30$ mm, and the range of sooting limits based on measurements using burneres at atmospheric pressure, drawn from the measurements of Takahashi and Glassman [17], Street and Thomas [18], Flossdorf and Wagner [19], and Calcote and Miller [20].

Present results for outwardly-progagating premixed flames suggest progressively increasing propensity to soot in the order ethylene, ethane, propylene, 1-3 butadiene and propane, based on progressively decreasing values of the critical fuel equivalence ratio at the sooting limit at atmospheric pressure. This ordering of the propensity of fuels to soot is identical to earlier findings of sooting limits for premixed flames stabilized on burners; thus, the main difference between the burner and outwardly-propagating spherical laminar premixed flame results is that the latter exhibit 10-15% larger critical fuel-equivalence ratios for the appearance of soot. This behavior probably is caused by reduced heat losses from the outwardly-propagating flames due to the absence of direct heat losses to burner surfaces which implies somewhat larger flame temperatures for the outwardly-propagating flames than for the burner-

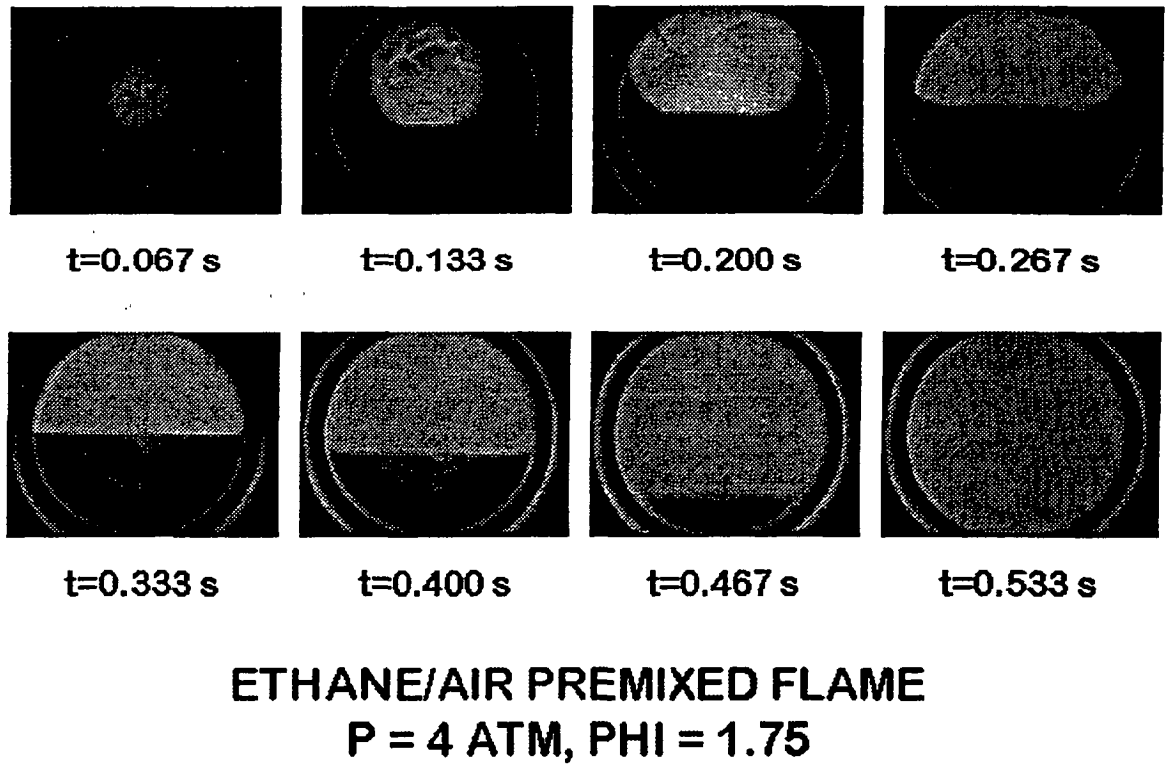

Fig. 4. Photographs of the development of buoyant soot-containing (ϕ=1.75) outwardly-propagating spherical laminar premixed flames (ethylene/air at 4 atm.).

stabilized flames at a given fuel-equivalence ratio. In particuler, it is widely recognized that increasing flame temperatures reduce the propensity of premixed flames to form soot [17-19].

Another interesting trend of the sooting limits illustrated in Figs. 5-9 is their progressive reduction with increasing pressure. In particular, values of the critical fuel equivalence ratio for the appearance of soot decease 4 - 17% as the pressure is increased in the range 0.5 - 4.0 atm, with the smallest reductions observed for fuels having the greatest propensity to soot. A surprising feature of this result is the rather small reduction of the critical fuel-equivalence ratio for the appearance of soot with nearly an order of magnitude increase of pressure, in view of other observations of a strong tendency for increasing pressure to increase soot concentrations and the propensity to emit soot from flames. For example, recent observations show that soot concentrations in diffusion flames increase by an order of magnitude for a pressure increase from 0.5 to 1.0 atm [30], whereas laminar smoke point flame lengths decrease somewhat more rapidly than the reciprocal of pressure [30].

Except for the ethylene/air flames, the results illustrated in Figs. 5-9 indicate that the buoyant limit is reached at a smaller fuel-equivalence ratio than the sooting limit. This behavior did not affect the determination of sooting limits, however, because yellow luminosity due to continuum radiation from soot appeared relatively early in the flame propagation process before the flames were significantly distorted by buoyancy. On the other hand, such buoyant effects would be a problem for studies of soot formation in outwardly-propagating spherical laminar premixed flames where larger post-flame regions are needed for detailed observations [1-16]. The problem of buoyancy occurs because fuel-rich soot-containing flames have relatively small flame speeds so that excessively large values of R are achieved a relativly small values of r_f. Problems of buoyancy, however, could be removed using one of the rapidly-developing microgravity techniques, see Refs. 40 and 41 and references cited therein.

As noted earlier, the sooting limits of all the present fuel/air mixtures are well within the preferential-diffusion unstable region where $Ma \leq 0$, based on the measurements of Hassan et al. [27]. Nevertheless, the appearance of chaotically disturbed fuel surfaces due to preferential-diffusion instability generally is deferred to larger values of fuel-equivalence ratio than the Ma = 0 limit at each pressure. This effect generally means that soot-containing outwardly-propagating spherical laminar premixed flames remain stable to preferential-diffusion effects for the flame sizes of interest ($r_f < 30$ mm) for pressures less than 1.5-2.0 atm. This behavior comes about because Markstein numbers do not reach very large negative values at low pressures so that instability effects remain relatively weak [27], whereas rates of development of chaotically distorted flame surfaces progressively decrease as the pressure decreases, as noted earlier. Avoiding the preferential-diffusion stability limitation for studies of soot formation in outwardly-propagating spherical laminar premixed flames at pressures greater than 1.5-2.0 atm might be

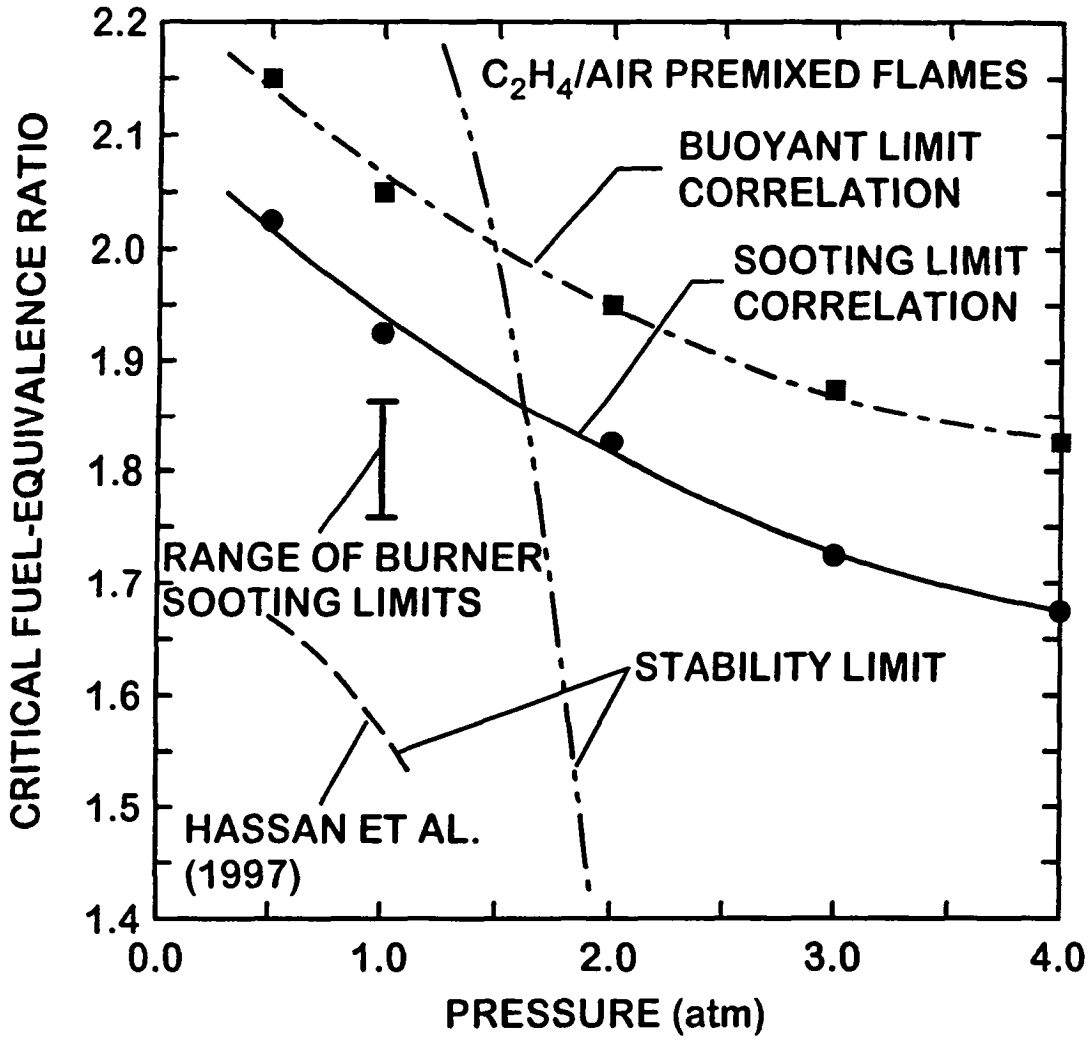

Fig. 5. Fuel-equivalence ratios at sooting, buoyant and preferential-diffusion stability limits as a function of pressure for outwardly-propagating spherical laminar premixed ethylene/air flames. Burner sooting limit results from Takahashi and Glassman [17], Street and Thomas [18], and Flossdorf and Wagner [19].

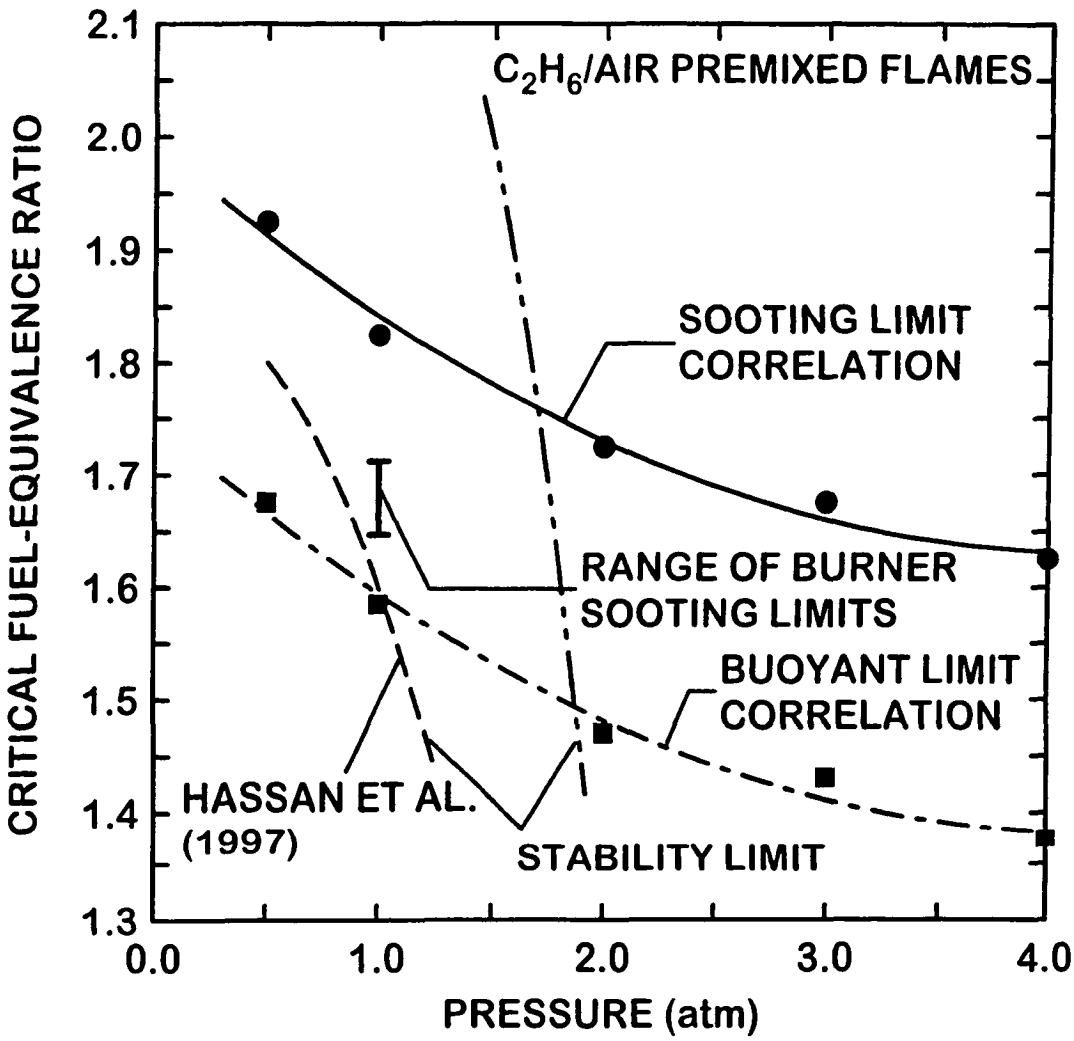

Fig. 6. Fuel-equivalence ratios at sooting, buoyant and preferential-diffusion stability limits as a function of pressure for outwardly-propagating spherical laminar premixed ethane/air flames. Burner sooting limit results from Takahashi and Glassman [17], Street and Thomas [18], and Flossdorf and Wagner [19].

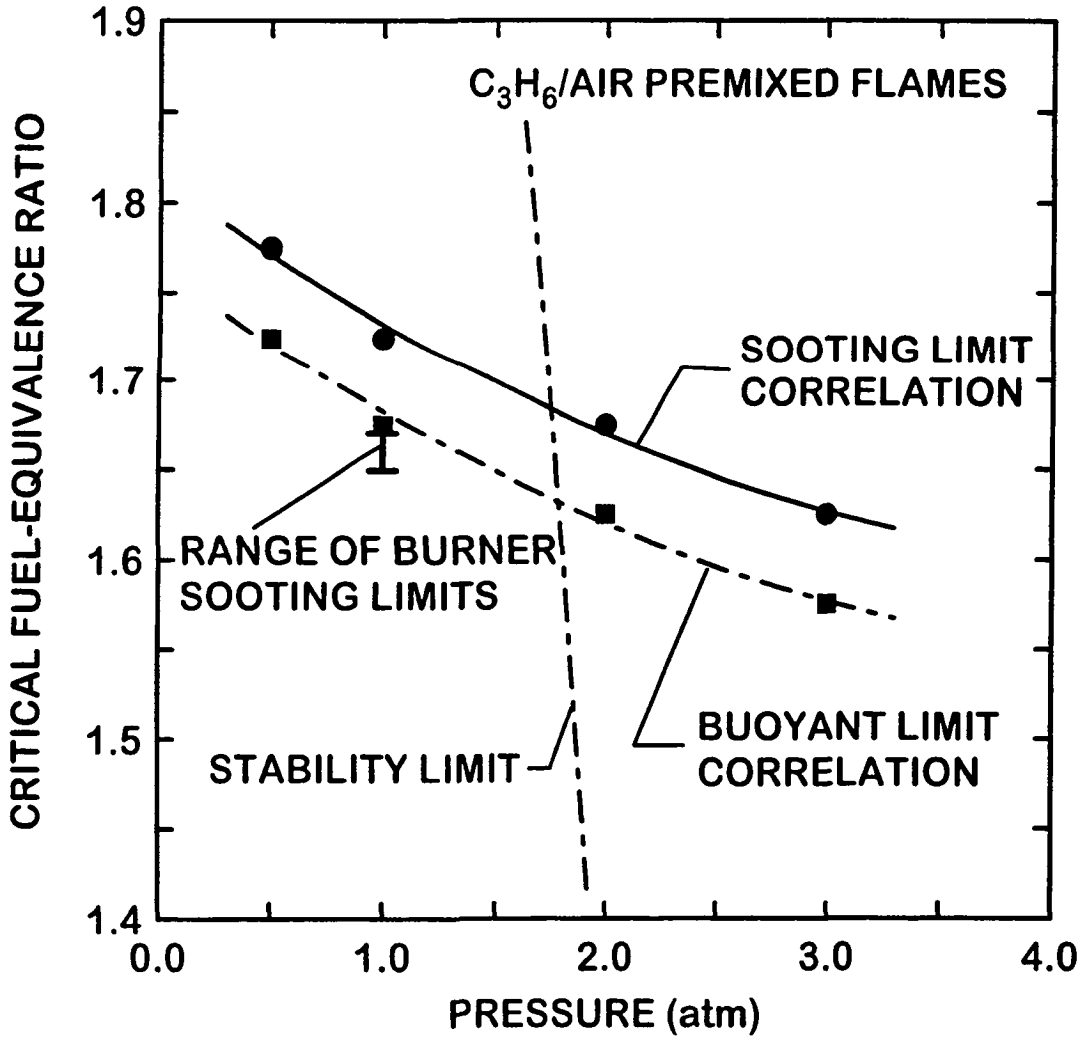

Fig. 7. Fuel-equivalence ratios at sooting, buoyant and preferential-diffusion stability limits as a function of pressure for outwardly-propagating spherical laminar premixed propylene/air flames. Burner sooting limit results from Takahashi and Glassman [17] and Street and Thomas [18].

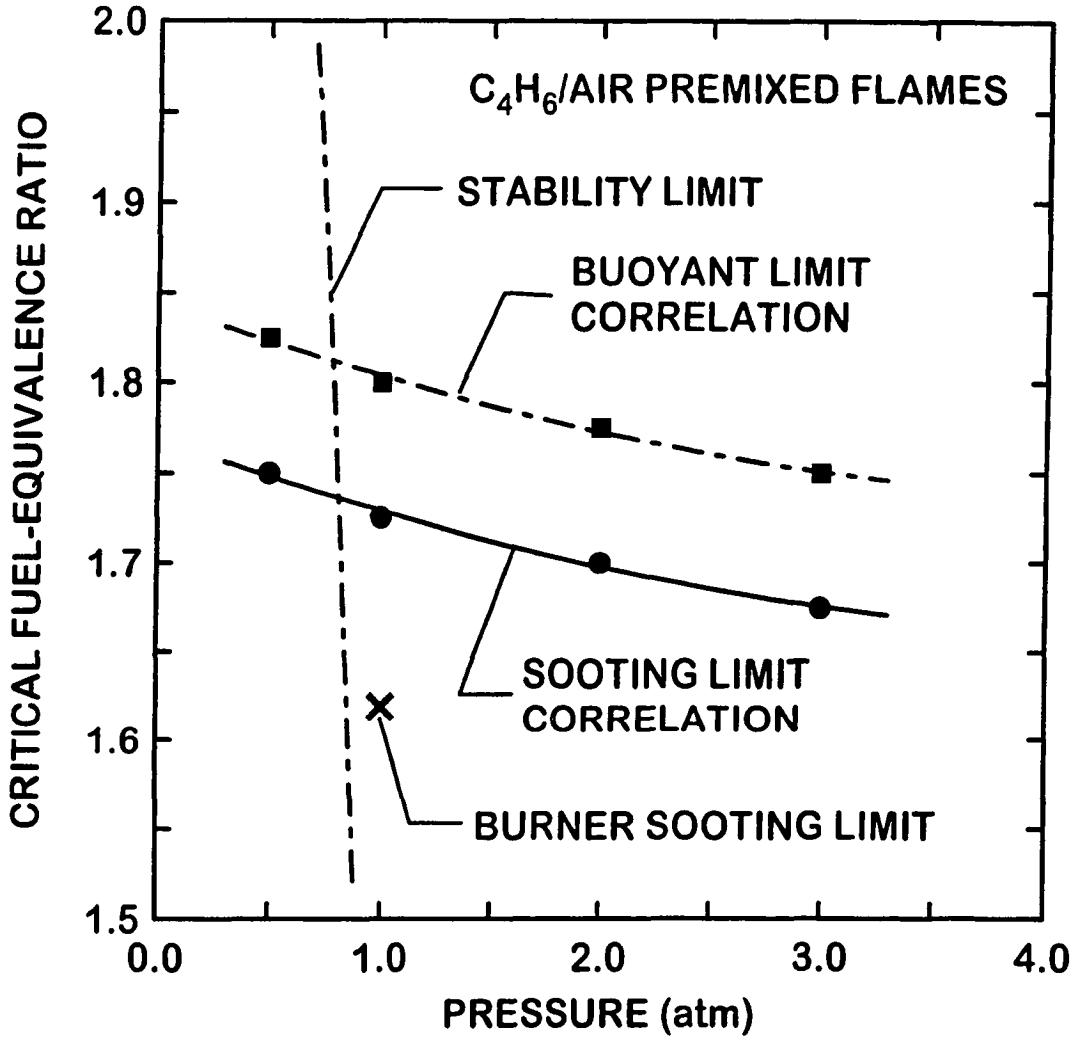

Fig. 8. Fuel-equivalence ratios at sooting, buoyant and preferential-diffusion stability limits as a function of pressure for outwardly-propagating spherical laminar premixed 1-3 butadiene/air flames. Burner sooting limit results from Takahashi and Glassman [17].

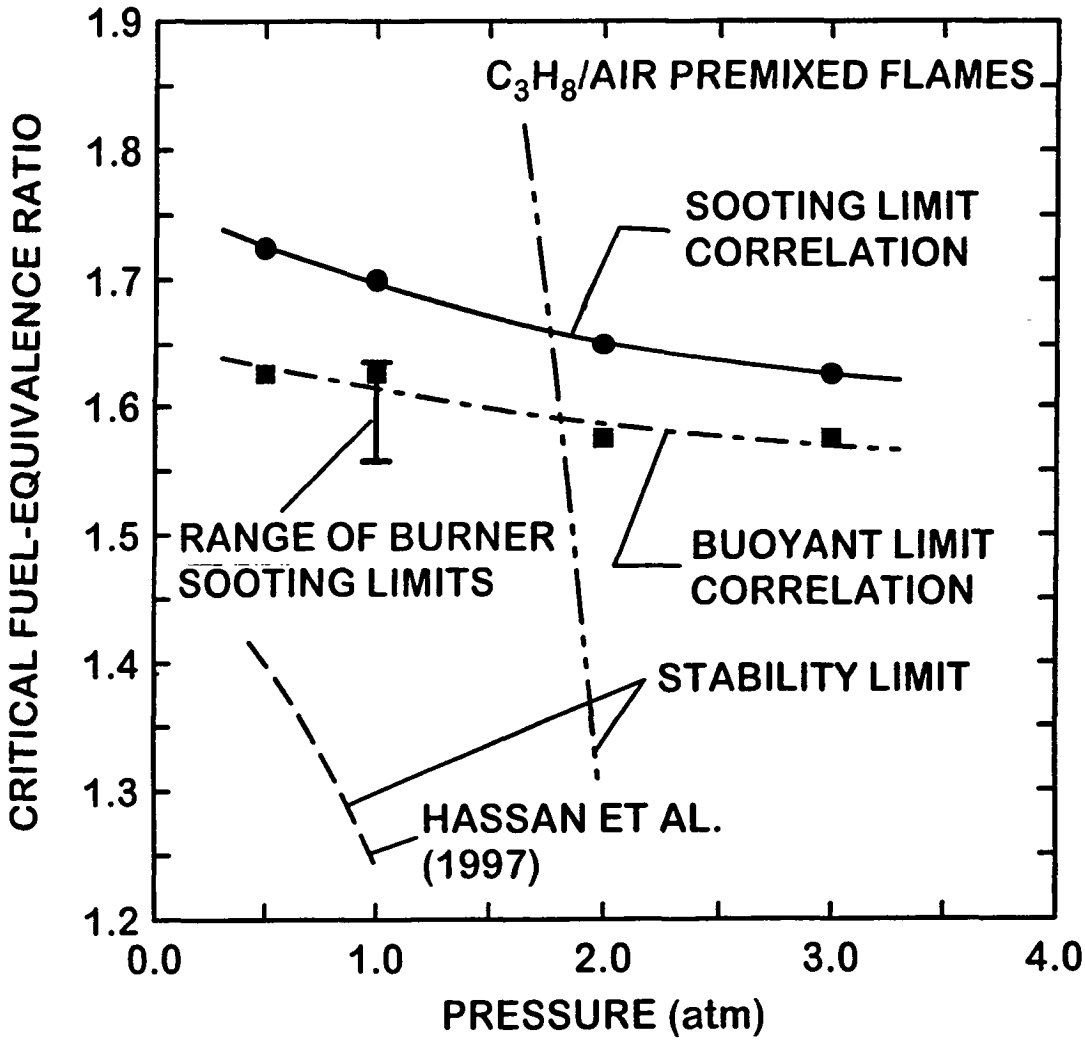

Fig. 9. Fuel-equivalence ratios at sooting, buoyant and preferential-diffusion stability limits as a function of pressure for outwardly-propagating spherical laminar premixed propane/air flames. Burner sooting limit results from Takahashi and Glassman [17], Street and Thomas [18], Flossdorf and Wagner [19] and Calcote and Miller [20].

possible using oxident mixtures other than air at room temperature. Due to the importance of a better understanding of soot processes at elevated pressures, studying such ways to avoid preferential-diffusion instability in soot-containing premixed flames at high pressures clearly merits additional attention.

2.6 Conclusions

Sooting limits, and flame stability with respect to effects of buoyancy and preferential diffusion, were studied for outwardly-propagating spherical laminar premixed flames fueled with ethylene, ethane, propylene, 1-3 butadiene and propane and burning in air at normal temperature and pressures of 0.5 - 4.0 atm. The major conclusions of the study are as follows:

1. Critical fuel-equivalence ratios for soot appearance progressively decrease in the order ethylene, ethane, propylene, 1-3 butadiene and propane which agrees with earlier burner observations at atmospheric pressure. Present measurements of critical fuel-equivalence ratios for soot appearance were 10-15% larger than the burner observations, however, which is attributed to effects of reduced heat losses compared to burner experiments.

2. Critical fuel-equivalence ratios for soot appearance decreased 4-17% as the pressure increased over the present test range, with the smallest decreases for fuels having the greatest propensity to soot. This reduction is surprisingly small in view of past observations of effects of pressure on soot concentrations in flames [40,41]; thus, the new results should provide an interesting test of future predictions of sooting limits.

3. Flame radii must be reasonably large (ca. 30 mm) in order to control unwanted effects of ignition disturbances and provide reasonable resolution to observe soot processes in outwardly-propagating spherical laminar premixed flames. Unfortunately, buoyant instabilities become problematical at these flame sizes before critical fuel-equivalence ratios for soot appearance are reached for fuel/air flames (except for ethylene/air flames) which means that these studies must be limited to low gravity conditions in most instances.

4. Preferential-diffusion instabilities appeared before reasonably large (ca. 30 mm) flame radii were reached for all soot-containing fuel/air flames at pressures greater than 1.5-2.0 atm. Unstable flames are not suitable for quantitative studies of soot processes; therefore, use of outwardly-propagating spherical laminar premixed fuel/air flames to study soot processes must be limited to pressures near and below atmospheric pressure in most instances.